

# Gene expression profile of hiPSC-derived cells differentiated with growth factors, forskolin and conditioned medium from human adrenocortical cell line

Ewelina Stelcer<sup>1,A–D</sup>, Karol Jopek<sup>1,B,C,F</sup>, Małgorzata Błatkiewicz<sup>1,B,C,F</sup>, Anna Olechnowicz<sup>1,2,B,C,F</sup>,  
Kacper Kamiński<sup>1,2,B,C,F</sup>, Marta Szyszka<sup>1,B,C,F</sup>, Wiktoria Maria Suchorska<sup>3,4,A,C,E</sup>, Marcin Ruciński<sup>1,A,C,E</sup>

<sup>1</sup> Department of Histology and Embryology, Poznan University of Medical Sciences, Poland

<sup>2</sup> Doctoral School, Poznan University of Medical Sciences, Poland

<sup>3</sup> Department of Electroradiology, Poznan University of Medical Sciences, Poland

<sup>4</sup> Radiobiology Lab, Greater Poland Cancer Centre, Poznań, Poland

A – research concept and design; B – collection and/or assembly of data; C – data analysis and interpretation;  
D – writing the article; E – critical revision of the article; F – final approval of the article

Advances in Clinical and Experimental Medicine, ISSN 1899–5276 (print), ISSN 2451–2680 (online)

*Adv Clin Exp Med.* 2024;33(4):397–407

## Address for correspondence

Ewelina Stelcer  
E-mail: ewelina.stelcer@ump.edu.pl

## Funding sources

National Science Centre grant No. UMO-2017/25/  
B//NZ4/00065

## Conflict of interest

None declared

Received on February 19, 2023

Reviewed on April 6, 2023

Accepted on June 20, 2023

Published online on August 4, 2023

## Cite as

Stelcer E, Jopek K, Błatkiewicz M, et al. Gene expression profile of hiPSC-derived cells differentiated with growth factors, forskolin and conditioned medium from human adrenocortical cell line. *Adv Clin Exp Med.* 2024;33(4):397–407. doi:10.17219/acem/168603

## DOI

10.17219/acem/168603

## Copyright

Copyright by Author(s)

This is an article distributed under the terms of the  
Creative Commons Attribution 3.0 Unported (CC BY 3.0)  
(<https://creativecommons.org/licenses/by/3.0/>)

## Abstract

**Background.** Adrenocortical carcinoma (ACC) affects approx. 2 in 1,000,000 individuals in the USA, and is more common in females than males. Adrenocortical carcinoma often presents with severe symptoms, such as abdominal pain, high blood pressure, acne, hair overgrowth, and voice deepening.

**Objectives.** Research on ACC constitutes a large body of published data. There is an increased need for easy access to ACC-derived biological material. Moreover, there are limited numbers of human cell lines available. For this reason, we attempted to differentiate human induced pluripotent stem cells (hiPSCs) into adrenocortical-like cells to establish a new functional cell line.

**Materials and methods.** We conducted a long-term differentiation process (35 and 70 days) in the presence of growth factors (GFs), forskolin and conditioned medium collected from the human adrenal carcinoma (HAC15) cell line. Then, we analyzed the gene expression profile of the differentiated cells.

**Results.** The obtained cells possess features characteristic of all 3 primary germ layers. Interestingly, the differentiated cells demonstrated an extremely high level of gene expression for those involved in endocrine processes, namely glycoprotein hormones, alpha polypeptide (CGA), insulin receptor substrate 4 (IRS4), and pancreatic progenitor cell differentiation and proliferation factor-like protein (PPDPFL).

**Conclusions.** The results of the study indicate that we obtained progenitors derived from endoderm with some characteristics of pancreatic-like cells. The endodermal derivative differentiation is a very challenging and complicated process; thus, the results presented in this study deserve closer consideration.

**Key words:** human induced pluripotent stem cells, endoderm, adrenal cells, forskolin

## Background

Adrenocortical tumors are quite frequent, with an incidence of 3–10% in the population.<sup>1</sup> These tumors can be divided into adrenocortical adenoma and adrenocortical carcinoma (ACC).<sup>2</sup> Adrenocortical carcinoma is sporadic, with a reported prevalence of 2 cases per 1,000,000 individuals/year, and is most frequently diagnosed in women (55–60% of cases) in their 4<sup>th</sup> or 5<sup>th</sup> decade of life.<sup>2,3</sup> The main substance currently approved for the treatment of ACC is mitotane (2,4'-dichlorodiphenyl)dichloroethane, 1-(2-chlorophenyl)-1-(4-chlorophenyl)-2,2-dichloroethane, with a recommended therapeutic plasma mitotane level of 14–20 mg/L (~50 µM).<sup>3</sup> However, the efficacy of this drug is limited due to its low pharmacokinetic properties and dose-limiting toxicity.<sup>3</sup>

Commercially available ACC human cell lines have a limited production capacity for mineralocorticoids, glucocorticoids and adrenal androgens. Furthermore, they show a limited response to angiotensin II (Ang II), adrenocorticotrophic hormone (ACTH) and potassium ions. Even so, they play an important role as a screening tool for cancer therapies.<sup>4,5</sup> Researchers mainly rely on 2 commonly used ACC cell lines, namely NCI-H295R and SW-13. Importantly, both cell lines are characterized by TP53 loss-of-function alterations.<sup>6</sup> Conversely to the non-hormone-producing SW-13 cells, NCI-H295R cells can produce steroid hormones and retain a gain-of-function Catenin beta 1 mutation.<sup>6,7</sup> A 3<sup>rd</sup> cell line, the human adrenal carcinoma (HAC15), can respond to Ang II, potassium and ACTH, being the first adrenal cell line capable of such responses.<sup>8</sup> Significant advances made in the last few years have changed the preclinical landscape for ACC. The new experimental models of ACC cells, namely MUC-1, CU-ACC1, CU-ACC2, JIL-2266, and TVBF-7, together with the commonly used NCI-H295R cell line, give researchers the instruments that are consistent with the well-defined heterogeneity of this disease and have the potential to disclose yet unknown patient subtype characteristics.<sup>9</sup> In particular, the usefulness of CU-ACC1 and CU-ACC2 cells as models to improve the search for targets and drug efficacy in the treatment of ACC has been demonstrated.<sup>10</sup> Nevertheless, there is a need to establish an ACC cell line that will show complete hormonal responses, steroidogenesis and expression of steroid-metabolizing enzymes.<sup>11</sup>

## Objectives

The objective of this study was to obtain cells that possess features of adrenal cells using human induced pluripotent stem cell (hiPSC) differentiation. We aimed to establish an easily accessible protocol, and for this reason, we relied on endo- and exogenous additives instead of previously described procedures, such as the overexpression of steroidogenic factor-1 (SF-1).<sup>12</sup> Because the cortex of the adrenal

gland is derived from mesoderm,<sup>13</sup> whereas the medulla is derived from the neural crest and is of ectodermal origin,<sup>14</sup> we decided to conduct long-term hiPSC differentiation via embryoid bodies (EBs) with all 3 primary germ layers for 35 days and 70 days in the presence of forskolin, growth factors (GFs) and conditioned media collected from the HAC15 cell line.

## Materials and methods

### Medium conditioning

A standard culture medium, consisting of Dulbecco's modified Eagle's medium/Nutrient Mixture F-12 (DMEM/F-12) (Thermo Fisher Scientific, Waltham, USA), 10% Cosmic Calf Serum (Hyclone; GE Healthcare, Westborough, USA) and 1% Insulin-Transferrin-Selenium (ITS) Premix Universal Culture Supplement (Corning Inc., Corning, USA), was used for conditioning. The medium was used for the HAC15 (ATCC® CRL-3301TM; American Type Cell Culture (ATCC), Manassas, USA) cells. The conditioned medium was collected after 24 h.

### Adrenal differential medium

Adrenal media consisted of DMEM/F-12, 10% fetal bovine serum (Biowest, Nuaillé, France), 10 µM of forskolin (Merck Millipore, Burlington, USA), 1% ITS Premix Universal Culture Supplement (Corning Inc.), 50 µM of ascorbic acid and 10<sup>-7</sup> M of dexamethasone (both from Merck Millipore), 10 ng/mL epidermal growth factor (EGF) and 10 ng/mL insulin-like growth factor 1 (IGF-1; both from STEMCELL Technologies, Cologne, Germany). All components of the medium were chosen based on previous adrenal-related literature.<sup>16–20</sup>

### hiPSC differentiation

We used 2 hiPSC cell lines, namely the purchased ND41658\*H (Coriell Cell Repository, Camden, USA) and GPCCi001-A, previously described by our group.<sup>21</sup> The cell lines formed EBs that were transferred onto 6-well plates coated with 0.1% gelatin (Merck Millipore, Darmstadt, Germany). On the 2<sup>nd</sup> day, the media were replaced with a 1:1 ratio of adrenal media and conditioned medium. The cells were collected 35 and 70 days after differentiation.

### Microarray study

The total RNA was isolated from both undifferentiated and differentiated hiPSC cell lines. The following variants were obtained: control (GPCCi001-A and ND41658\*H pooled into one) (i), 35 days differentiation (ii) and 70 days differentiation (iii). The whole procedure of preparing RNA for hybridization was conducted using the GeneChip™

WT PLUS Reagent Kit (Affymetrix Inc., Santa Clara, USA). The complete procedure has been described previously.<sup>22–26</sup> Briefly, a two-step cDNA synthesis reaction was carried out with 100 ng of RNA using random primers extended by the T7 RNA polymerase promoter sequence. The cRNA was synthesized by the in vitro transcription for 16 h at 40°C. Then, the cRNA was purified and re-transcribed into cDNA. Next, the cDNA was biotin-labeled and fragmented using the Affymetrix GeneChip WT Terminal Labeling and Hybridization kit (Affymetrix Inc.). Biotin-labeled fragments of cDNA were hybridized using the Affymetrix Human Gene 2.1 ST ArrayStrip (20 h, 48°C), and the microarrays were stained with the aid of the Affymetrix GeneAtlas Fluidics Station (Affymetrix Inc.). Finally, the array strips were scanned using a GeneAtlas Imaging Station (Thermo Fisher Scientific). The preliminary analysis of the scanned chips was carried out with the use of Affymetrix GeneAtlas Operating Software (Affymetrix Inc.), and the quality of gene expression data was verified using the software's quality control criteria.

The obtained CEL files were analyzed using the R statistical language (R Foundation for Statistical Computing, Vienna, Austria) and Bioconductor package, including the selected Bioconductor libraries. The Robust Multi-array Average (RMA) normalization algorithm implemented in the “Affy” library was applied for the normalization, background correction and calculation of the expression values of the analyzed genes. A complete gene data table, including normalized gene expression values, gene symbols, gene names, and Entrez IDs was prepared based on the assigned biological annotations taken from the pd.hugene.2.1.st library. Linear microarray data models with moderated t statistics included in the “limma” library were applied for the expression and statistical assessment. The established cutoff criteria were as follows: the absolute value of expression fold change (FC) >2 and false discovery rate (FDR) adjusted  $p \leq 0.01$ . Genes fulfilling those criteria were considered differentially expressed genes (DEGs) and were subjected to further analyses. The result of such selection was presented as a volcano plot, showing the total number of up- and downregulated genes.

Variances were calculated for the entire gene expression dataset, and the top 1000 genes with the highest variance were subjected to principal component analysis (PCA). Principal component analysis of gene expression dataset was performed and visualized using factoextra library<sup>27</sup> with default parameters ( $n = \text{“auto”}$ ,  $\text{rotation} = \text{“none”}$ ,  $\text{center} = \text{TRUE}$ ,  $\text{scale} = \text{TRUE}$ ).

The entire set of DEGs was subjected to functional annotation and clustering using the Database for Annotation, Visualization, and Integrated Discovery (DAVID) bioinformatics tool.<sup>28</sup> All gene IDs of DEGs were uploaded to DAVID with the use of the RDAVIDWebService Bioconductor library,<sup>29</sup> where they were assigned to relevant Gene Ontology (GO) terms, with a subsequent selection

of significantly enriched GO terms from the GO BP FAT database. The kappa statistics p-values of selected GO terms were corrected using Benjamini–Hochberg procedure, and were described as adjusted p-values. Differentially expressed genes from each comparison were visualized with a heatmap using the ComplexHeatmap library.<sup>30</sup>

Gene set enrichment analysis (GSEA) was carried out using the clusterProfiler Bioconductor library.<sup>31</sup> The analysis aimed to identify the level of depletion or enrichment in GO terms by calculating normalized enrichment score (NES) with a relevant p-value. Normalized FC values from all genes were  $\log_2$ -transformed, sorted and used as an argument for the gseGO function. The gene set enrichment was performed regarding the “biological process” GO category, assuming the minimum size of each geneSet for analyzing = 100 and Fisher exact p-value  $\leq 0.001$ . Ten ontology groups with the highest enrichment score (the highest NES value) and 10 groups with the most depleted enrichment score (the lowest NES value) were visualized in a bar chart. Enrichment plots for 5 of the most enriched and 5 of the most depleted GO terms were also presented.

Technical descriptions with raw and normalized data files were deposited in the Gene Expression Omnibus (GEO) repository at the National Center for Biotechnology Information (<http://www.ncbi.nlm.nih.gov/geo/>), under the GEO accession No. GSE150775.

## Real-time quantitative polymerase chain reaction analysis

Real-time quantitative polymerase chain reaction (qPCR) was carried out using the PrimePCR™ SYBR® Green Assay (Bio-Rad, Hercules, USA) and the specific synthesized primers for pancreatic progenitor cell differentiation as well as glycoprotein hormones, alpha polypeptide (CGA), and insulin receptor substrate 4 (*IRS4*).

## Immunohistochemistry

After 70 days of differentiation, GPCCi001-A cells were fixed using 4% phosphate-buffered formalin, embedded in paraffin and sectioned. The samples were then stained using anti-CGA (ABIN3021817, 1:200) and anti-pancreatic progenitor cell differentiation and proliferation factor-like protein (PPDPFL) (NBP2-31818, 1:20) antibodies, according to the manufacturer's instructions.

## Results

The 2 hiPSC cell lines undergoing 70-day differentiation changed their morphology during differentiation in vitro from cells forming colonies of EBs to spindle-like cells (Fig. 1A,B). Furthermore, they demonstrated active



proliferation during differentiation. The morphology of both differentiated hiPSC-derived cell lines was very similar.

To perform a complete comparison of differentiated cells and hiPSC transcriptomic profiles, we analyzed whole genome expression using Affymetrix Human Gene 2.1 ST ArrayStrips. Principal component analysis (Supplementary Fig. 1A) indicated clear segregation of cells before and after differentiation. After both 35-day and 70-day differentiation, there were distinct groups of hiPSCs visible. Moreover, both differentiation time points shared 30.7% of upregulated and 27.5% of downregulated genes, which corresponds to 47 and 56 genes, respectively (Supplementary Fig. 1B).

The general profile of whole gene expression in the differentiated ND41658\*H/GPCCi001-A and undifferentiated groups is shown in a volcano plot (Fig. 2A), with each dot representing the mean expression level ( $n = 3$ ) of a single gene obtained from a microarray normalized dataset. The selection criteria aimed at determining significantly altered gene expression were based on the absolute expression fold difference  $>2$  and an adjusted  $p \leq 0.01$ . Genes above the cutoff value are differentially expressed and presented as orange (downregulated genes) or blue (upregulated genes) dots. Based on these criteria, 62 genes were significantly downregulated, and 100 genes were upregulated in the differentiated group compared to the hiPSCs 70 days after differentiation. Ten genes with the highest and 10 genes with the lowest FC values are presented in table format displaying the gene symbol, gene name, FC, and adjusted p-value (Fig. 2B). These genes were characterized by high FC values, especially for upregulated genes (range for upregulated genes: 79.90–5.89, and for downregulated genes: –5.76––2.98). This group

of genes includes glycoprotein hormones, namely *CGA* (FC = 79.90), *IRS4* (FC = 22.31), phosphoenolpyruvate carboxykinase 1 (*PCK1*) (FC = 7.24), synaptotagmin-like 5 (*SYTL5*) (FC = –5.76), Kelch-like family member 4 (*KLHL4*) (FC = –4.56), and gamma-aminobutyric acid type A receptor subunit epsilon (*GABRE*) (FC = –4.41).

We also compared gene expression profiles of cells after 35 days of differentiation to hiPSCs, and 70 days to 35 days after differentiation (Supplementary Fig. 2A,B). Interestingly, in 35-day cells, the high expression of *CGA*, *IRS4* and *PPDPFL* was notable. We found 198 genes significantly downregulated, and 99 were upregulated in the treated group compared to the hiPSCs 35 days after differentiation. The 2<sup>nd</sup> stage of differentiation (day 70 compared to day 35) resulted in minimal gene expression changes. No genes were downregulated and 8 genes were upregulated.

A bioinformatic evaluation of transcriptomic modulation was performed using GSEA (Fig. 3). This approach was based on the full transcriptomic profile analysis, regardless of the predefined cutoff criteria (FC  $> 2$ ,  $p \leq 0.01$ ). In this method, genes pre-ranked by logarithmic FC values were employed to determine enrichment (positive NES) or depletion (negative NES) in the GO-BP database after hiPSC differentiation. The largest cluster of enriched or depleted terms was related to “cell GTPase cell-cell involved”, “histone internal peptidyl-lysine acetylation”, “hormone-mediated intracellular steroid hormone”, “regulation of mRNA metabolic process” and “anion chloride transport” (Fig. 3A).

The 70-day differentiation led to the enrichment of genes involved in the regulation of steroid biosynthetic process (NES: 2.436), endocrine process (NES: 2.304) and mitochondrial adenosine triphosphate (ATP) synthesis coupled electron transport (NES: 2.328), as well as to the depletion

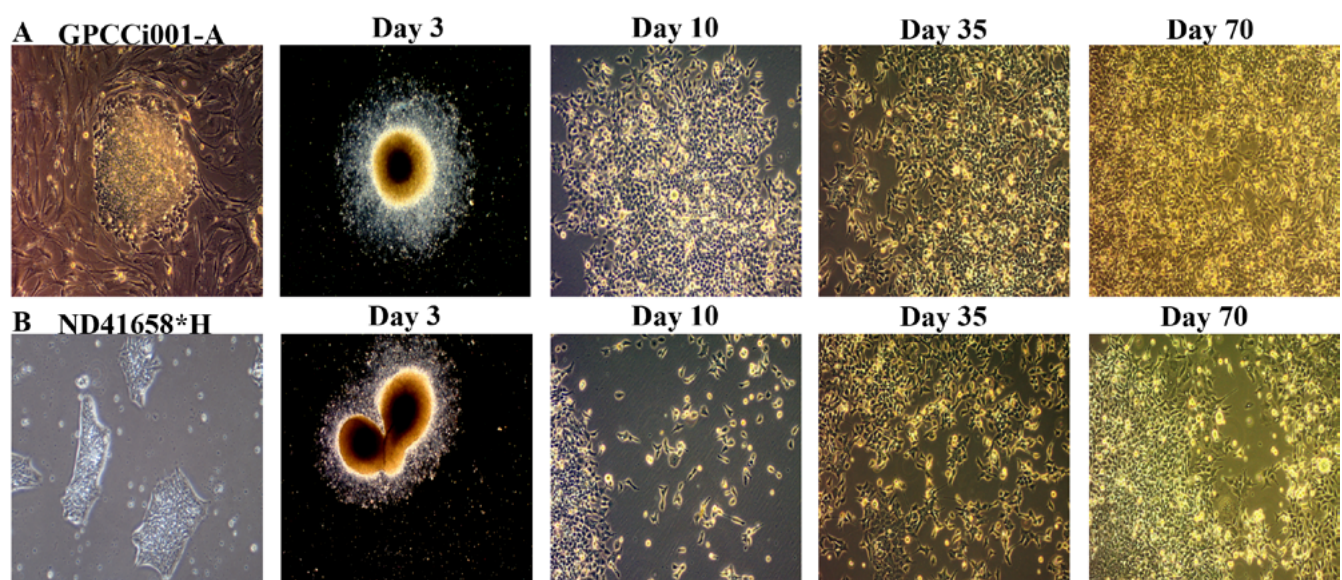


**Fig. 1.** Two human induced pluripotent stem cell (hiPSC) cell lines: GPCCi001-A (A) and ND41658\*H (B), were differentiated via embryoid bodies (EBs) for 70 days in the presence of growth factors (GFs): epidermal growth factor (EGF) and insulin-like growth factor 1 (IGF-1), forskolin and conditioned medium collected from a human adrenal carcinoma (HAC15) cell line. They lost the ability to form colonies and took a spindle-like shape

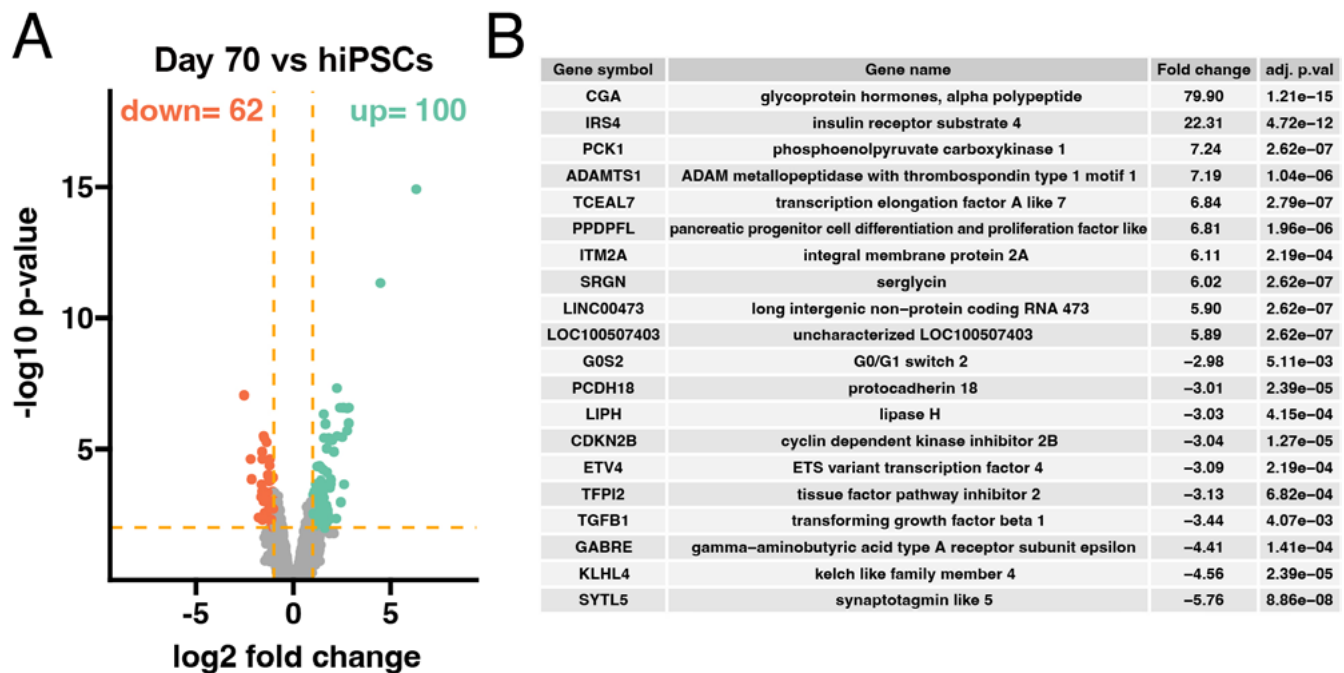


**Fig. 2.** The general profile of whole gene expression in the differentiated ND41658\*H/GPCCI001-A and undifferentiated (untreated ND41658\*H/GPCCI001-A) groups is shown in a volcano plot (A), with each dot on the graph corresponding to 1 transcript. Genes above the cutoff value are differentially expressed and shown as orange (downregulated genes) or blue (upregulated ones) dots. Seventy days after differentiation, 62 genes were significantly downregulated, and 100 genes were upregulated in the differentiated group compared to the human induced pluripotent stem cells (hiPSCs). Ten genes with the highest and 10 genes with the lowest fold change (FC) values are presented in tabular format displaying the gene symbol, gene name, FC, and adjusted p-value (B)

of genes related to, e.g., hormone-mediated signaling pathway (NES: -2.050), chloride transport (NES: -2.088) and histone H3-K4 methylation (NES: -2.155), among others (Fig. 3B).

The GSEA analysis also showed a significant decrease in the expression of genes closely related to cell–cell junction organization and intracellular steroid hormone receptor signaling pathway. These groups are comprised of genes with very low logFC values, thus their expression is suppressed during differentiation (Fig. 3C).

The interaction network between genes with the highest impact on “endocrine process”, “regulation of steroid biosynthetic process” and “mitochondrial respiratory chain complex” is presented in Fig. 3D. The expression of all presented genes increased after differentiation, suggesting that this process affects the physiological function of hiPSCs in a hormone-dependent manner.

Then, GO terms were assigned to the DEGs (Fig. 4). The GO analysis showed that the differentiation of hiPSCs significantly alters the expression of certain genes that play an essential role in the regulation of transcription, DNA-templated (GO: 0006351), regulation of vascular development (GO: 1901342), regulation of angiogenesis (GO: 0045765), epithelium development (GO: 0060429), cell death (GO: 0008219), and blood vessel development (GO: 0001568). Interestingly, at the differentiation midpoint (day 35), we observed a large decrease in the expression of genes involved in response to growth factor (GO: 0070848), regulation of cell communication (GO:

0010646), circulatory system development (GO: 0072359), cell migration (GO: 0016477), and blood vessel development (GO: 0001568). This suggests that circulatory-like features are developed in cells after 35 days of differentiation. The comparison between day 70 and day 35 did not show crucial gene expression changes.

Due to the structure of the GO database, single genes can often be assigned to many ontological terms. For this reason, the relationship between genes and GO terms with visualization of logFC values and gene symbols was demonstrated. To better show all dependencies, the results were compiled in a heatmap involving gene expression of all groups (day 70 compared to hiPSCs, day 35 compared to hiPSCs and day 70 compared to day 35) (Supplementary Fig. 3).

We also investigated the expression of genes involved in the 3 primary germ layers and stemness using qPCR *GATA4* (FC = 1.98,  $p \leq 0.05$ ) as an endodermal marker,  $\alpha$ -smooth muscle actin ( $\alpha$ -SMA) (FC = 0.28,  $p \leq 0.001$ ) and Brachyury as mesodermal markers, Vimentin and paired box 6 (*PAX6*) (FC = 0.872,  $p > 0.05$ ) as ectodermal markers, as well as *CD133* (FC = 0.61,  $p \leq 0.05$ ), *CD117* (FC = 0.989,  $p > 0.05$ ), *CD44* (FC = 0.46,  $p \leq 0.01$ ), and SRY-box transcription factor 2 (*SOX2*) (FC = 0.639,  $p > 0.05$ ) as stem and/or cancer cell markers after 70-day differentiation (Supplementary Fig. 4). To confirm or refute our hypothesis, we have also examined features characteristic of adrenocortical-like cells. After 70 days of differentiation, the cells did not demonstrate expression of markers characteristic of adrenal cells such as steroidogenic acute

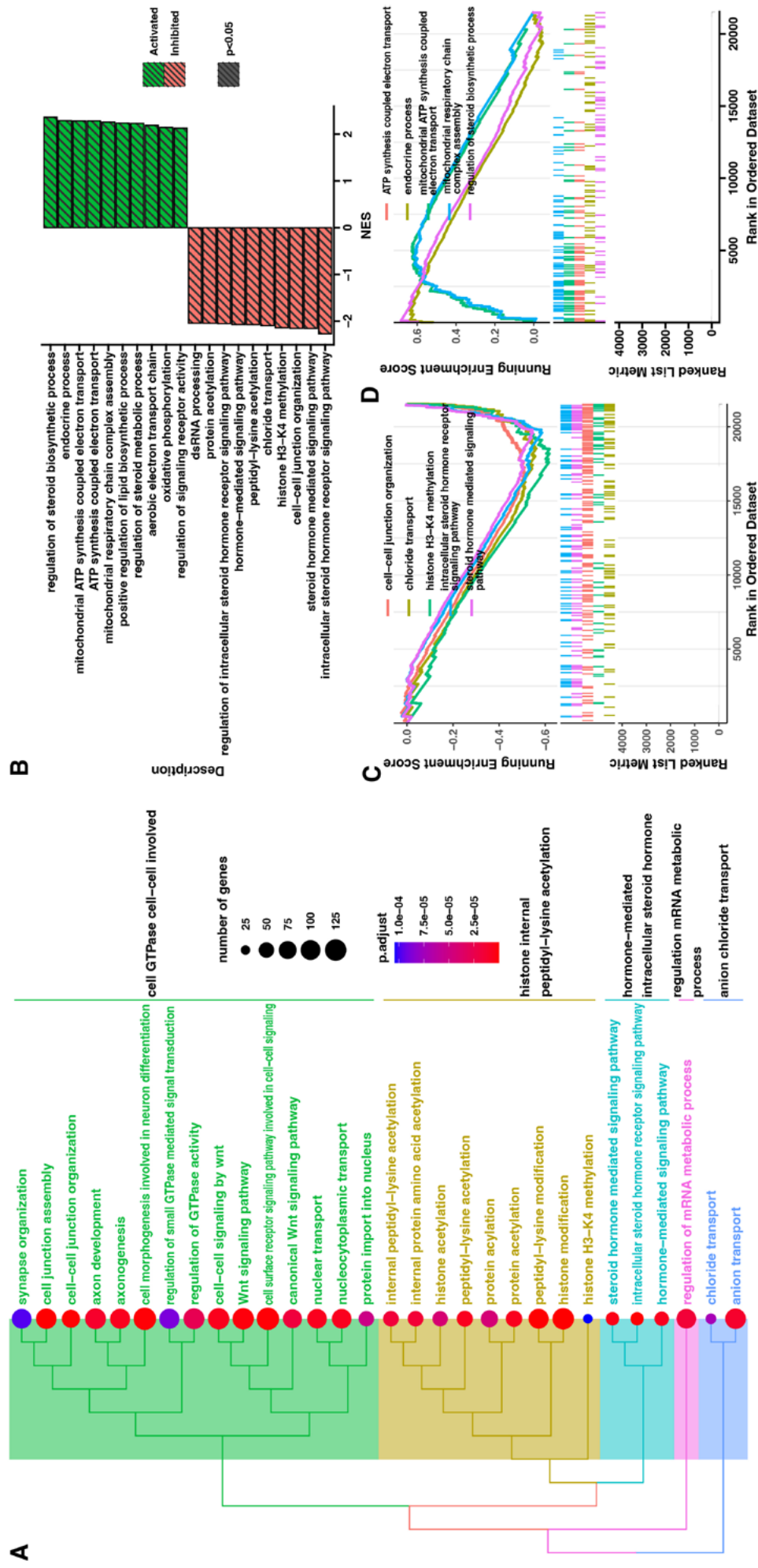


**Fig. 3.** A bioinformatic evaluation of transcriptome modulation was performed using gene set enrichment analysis (GSEA). Genes pre-ranked using logarithmic fold change (FC) values were employed to determine enrichment (positive normalized enrichment score (NES) or depletion (negative NES)) in the GO-BP database. The largest cluster of enriched or depleted terms was related to “cell GTPase cell-cell involved”, “histone internal peptidyl-lysine acetylation”, “hormone-mediated intracellular steroid hormone”, “regulation mRNA metabolic process”, and “anion chloride transport” (A). Differentiation of cells led, i.e., to the enrichment of genes involved in the regulation of steroid biosynthetic process and endocrine process, and to the depletion of genes related to, e.g., hormone-mediated signaling pathway (B). GSEA analysis also showed a significant decrease in the expression of genes closely related to cell-cell junction organization and intracellular steroid hormone receptor signaling pathway (C). The interaction network between genes with the highest impact on, i.e., endocrine process and regulation of steroid biosynthetic process are presented (D)

ATP – adenosine triphosphate.





**Fig. 4.** Differentially expressed genes from an investigated group (day 70 compared to human induced pluripotent stem cells (hiPSCs)) were then assigned to Gene Ontology (GO) terms. The GO analysis showed that differentiation alters the expression of genes that play an essential role in the regulation of signaling pathways, e.g., regulation of vascular development, regulation of angiogenesis, epithelium development, and blood vessel development. Halfway through differentiation (day 35), a high decrease in the expression of genes involved in, i.e., response to growth factor, regulation of cell communication, circulatory system development, cell migration, and blood vessel development was observed

regulatory protein (*STAR*), cytochrome P450, family 11, subfamily A, polypeptide 2 (*CYP11A2*), or cytochrome P450 family 11 subfamily B member 2 (*CYP11B2*) (data not shown), and based on enzyme-linked immunosorbent assay (ELISA), they did not secrete the primary hormones involved in steroidogenesis (aldosterone and cortisol; data not shown). The most upregulated genes, *CGA* and *IRS4*, were subjected to further qPCR evaluation in both hiPSCs cell lines separately (Supplementary Fig. 5A,B). The differentiated hiPS ND41658\*H cells demonstrated elevated gene expression of *CGA* (FC = 573.6,  $p > 0.05$ ) and *IRS4* (FC = 255.5,  $p \leq 0.01$ ). In turn, hiPS GPCCi001-A cells were characterized by increased gene expression levels of *CGA* (FC = 564,  $p \leq 0.05$ ) and *IRS4* (FC = 220.2,  $p \leq 0.05$ ) after 70 days of differentiation. Based on these data, we confirmed the expression of *CGA* and *PPDPFL* at the protein level using immunohistochemistry in the hiPSC GPCCi001-A cell line, revealing statistical significance in the case of both *CGA* and *IRS4* gene expression levels (Supplementary Fig. 5C).

## Discussion

Adrenocortical carcinoma research constitutes a large body of published data, although there is only limited information available on human cell lines. Therefore, there is still a strong need to establish a functional ACC cell line. The main aim of this study was to obtain cells with features characteristic of adrenal cells via long-term differentiation in vitro. To verify our hypothesis, 2 hiPSC cell lines were subjected to differentiation in the presence of GFs, forskolin and ACC-conditioned medium (Fig. 1). The gene expression profile of differentiated cells differs significantly from undifferentiated and partially differentiated hiPSCs (Supplementary Fig. 1,2). Our findings demonstrated that instead of adrenocortical-like cells, we obtained cells with some endodermal features. Below, we discuss our results in the context of the differentiation of stem cells (SCs) into endodermal precursors and adrenocortical-like cells (originating from mesoderm).

Yazawa et al. revealed that mesenchymal stem cells (MSCs) can be differentiated into steroidogenic cells by expressing nuclear receptor 5A subfamily proteins (SF-1 and liver receptor homolog-1 (LRH-1)) in the presence of cyclic adenosine monophosphate (cAMP).<sup>32</sup> Notably, the authors highlighted that there is a strong need to establish efficient protocols for inducing SF-1 and LRH-1 expression in SCs without gene transfer.<sup>32</sup>

Another interesting approach was demonstrated by Li et al., who differentiated hiPSCs into adrenal cells with high efficiency toward androgen-producing Leydig cells.<sup>33</sup> They used 2 systems, namely MesenCult™-ACF Attachment Substrate-coated plates for generating adrenal cells

and plates coated with Collagen I rat protein solution for obtaining Leydig cells. These 2 systems involve deriving mesenchymal progenitors and overexpression of SF-1 in the presence of dibutyryl-cAMP, desert hedgehog and human chorionic gonadotropin.<sup>33</sup>

Sonoyama et al. differentiated human embryonic stem cells (hESCs) and hiPSCs into steroid-producing cells involving the multistep method.<sup>12</sup> First, SCs were differentiated into the mesodermal lineage cells with the aid of BIO, a glycogen synthase kinase-3 beta inhibitor. Then, the mesodermal cells were transfected with plasmid DNA which encodes SF-1. The transfectants were further differentiated under the addition of 8-bromoadenosine 3',5'-cyclic monophosphate.<sup>12</sup>

The aforementioned studies show that the majority of protocols are based on forced overexpression of SF-1 in SCs. Our aim was to obtain adrenocortical-like cells without using genetic engineering tools. We focused on the influence of ACC-conditioned medium and exogenous addition of adrenal-related factors to the hiPSC-derived EBs. As a result, the cells acquired spindle-like morphology after long-term differentiation (Fig. 1) and were characterized by an altered gene expression profile (Fig. 2). They did not demonstrate the expression of genes involved in steroidogenesis (Supplementary Fig. 3) and did not secrete hormones after stimulation. Based on that, we can assume that our cells do not possess the features of adrenocortical cells.

The endodermal cells are challenging to grow in vitro, while the acquisition of primary tissues is often problematic and ethically questionable, especially from healthy donors. Consequently, basic research, disease modeling and regenerative medicine applications are limited by the lack of high-quality endodermal cells. Thus, the production of endodermal derivatives has been a major focus in the field of human pluripotent stem cells (hPSCs) for over 20 years.<sup>15</sup>

Organs derived from definitive endoderm, like the pancreas, are of great interest. Thus, D'Amour et al. described the production of enriched cultures of definitive endoderm derived from hESCs in the presence of activin A and low serum.<sup>34</sup> The transplantation of these cells under the kidney capsule resulted in their further differentiation into more mature cells with characteristics of endodermal organs.<sup>34</sup>

Moreover, Bogacheva et al. demonstrated the influence of biomaterial properties on the endodermal differentiation process and the importance of spheroid size control for successful hiPSC differentiation.<sup>35</sup> The spheroid size determines the availability of growth factors as well as the supply of nutrients and oxygen to all cells. Suspension culture ensures sufficient mass transfer and thus provides more effective definitive endoderm differentiation in the presence of B-27 and activin A than nanofibrillar cellulose hydrogel-based culture.<sup>35</sup>



Kopper and Benvenisty differentiated hESC-derived EBs into endodermal progenitors in the presence of activin A and fibroblast growth factor-2 (FGF2).<sup>36</sup> According them, once endoderm progenitor cells are isolated from other cell types and create their niche, they differentiate into hepatic, bile and colon tissues.<sup>36</sup>

Fang and Li described a simplified but highly efficient procedure to induce hESC-based endoderm differentiation with crotonate, a precursor of crotonyl-CoA for histone crotonylation deposition on endodermal genes.<sup>37</sup> In this method, the addition of crotonate in different endodermal differentiation media significantly improved the differentiation efficiency and substantially diminished the number of required reagents.<sup>37</sup>

A protocol based on the addition of all-trans-retinoic acid, basic FGF and dibutyryl-cAMP may result in obtaining definitive endoderm from murine ESCs in the absence of EB formation. Those cells may serve as pancreatic precursors and display an increased SOX17 and FOXA2 expression, consistent with definitive endoderm production.<sup>38</sup>

To understand the distinctions between endodermal derivatives and other lineage-specific progenitors, the transcriptomes of 2-day mouse embryonic stem cells (mESCs) differentiated with bone morphogenetic protein 4 (BMP4), activin A and CHIR99021 were examined with scRNA-seq. The analysis revealed an endodermal-specific signature that is enriched for NODAL and Wntless-INT (WNT) signaling pathways, as well as metabolism-related gene expression.<sup>39</sup>

Based on those studies, we believe that our results are of high scientific quality. Since differentiation toward mesodermal lineage was not our primary aim, we did not use activin A and FGF, which seems to be crucial in endodermal differentiation. On the contrary, the use of ACC-conditioned medium, forskolin, ascorbic acid, dexamethasone, EGF, and IGF-1 resulted in extremely high expression of genes characteristic for pancreatic-like cells, namely *CGA*, *IRS4* and *PPDPFL* (Fig. 2 and Supplementary Fig. 3). Moreover, we have demonstrated the presence of those markers at the protein level (Supplementary Fig. 5). Notably, our results indicate that signaling pathways connected with the circulatory system originating from mesoderm are activated in the obtained cells (Fig. 3,4). However, the qPCR analysis did not confirm higher expression of mesodermal markers  $\alpha$ -SMA and Brachyury (Supplementary Fig. 4), and thus in this study, we focus on endodermal-like properties, which are more challenging to induce.

## Limitations

We are aware that the results presented in this study are contrary to the assumed hypothesis. Nevertheless, we demonstrated comprehensive research, which provides new knowledge in the fields of cell biology and regenerative medicine. Apart from that, the in vitro research should be confirmed through in vivo experiments.

## Conclusions

Herein, we presented an interesting outcome of long-term hiPSC differentiation in the presence of a conditioned medium collected from human ACCs, forskolin and other GFs. The gene expression profile revealed that obtained cells had features of all primary germ layers. We revealed that the gene expression profile of cells following 70-day differentiation differs from those differentiated for 35 days, as well as from undifferentiated hiPSCs. Moreover, we observed the elevated expression of endodermal markers like GATA Binding Protein 4 (GATA4). In the near future, they may have the potential to serve as endoderm precursors, such as pancreatic-like cells. Because the differentiation of SCs into endodermal derivatives is a challenging task, we believe that the work presented in our study will contribute to the improvement in generating specialized hiPSC-derived cells. Those cells could constitute a promising approach to tissue engineering in the future.

## Supplementary data

The supplementary materials are available at <https://doi.org/10.5281/zenodo.7933236>. The package contains the following files:

Supplementary Fig. 1. PCA (A) indicates clear segregation of cells before and after differentiation. Cells after 35-day and 70-day differentiation create groups very distinct from hiPSCs. It is also noticeable that cells at both differentiation time points share 30.7% of upregulated and 27.5% of downregulated genes (B).

Supplementary Fig. 2. 35 days after differentiation, 198 genes were significantly downregulated and 99 were upregulated in the treated group compared to the hiPSCs (A). The 2<sup>nd</sup> stage of differentiation (day 70 compared to day 35) resulted in barely noticeable gene expression changes: 0 genes were downregulated and 8 genes were upregulated (B).

Supplementary Fig. 3. The connection between genes and GO terms with visualization of logFC values and gene symbols was demonstrated. To better show all dependencies, those results were compiled in a heatmap involving gene expression of all compared groups (day 70 compared to hiPSCs, day 35 compared to hiPSCs and day 70 compared to day 35).

Supplementary Fig. 4. GATA4 (FC = 1.98,  $p \leq 0.05$ ) as an endodermal marker (i),  $\alpha$ -SMA (FC = 0.28,  $p \leq 0.001$ ) and Brachyury as mesodermal markers (ii), vimentin and PAX6 (FC = 0.872,  $p > 0.05$ ) as ectodermal markers (iii), as well as CD133 (FC = 0.61,  $p \leq 0.05$ ), CD117 (FC = 0.989,  $p > 0.05$ ), CD44 (FC = 0.46,  $p \leq 0.01$ ), SOX2 (FC = 0.639,  $p > 0.05$ ) as stem and/or cancer cell markers (iv) after 70-day differentiation. The median, interquartile range (IQR) and mean (as diamond) are marked on the plots.

Supplementary Fig. 5. The most upregulated genes, *CGA* and *IRS4*, were subjected to further qPCR evaluation in both hiPSC cell lines separately (A,B). The differentiated hiPS ND41658\*H cells demonstrated elevated gene expression as follows: *CGA* (FC = 573.6,  $p > 0.05$ ) and *IRS4* (FC = 255.5,  $p \leq 0.01$ ). The hiPS GPCCi001-A cells after 70-day differentiation were characterized by increased gene expression levels in the following manner: *CGA* (FC = 564,  $p \leq 0.05$ ) and *IRS4* (FC = 220.2,  $p \leq 0.05$ ). Based on that, we confirmed the expression of CGA and PPDPFL at the protein level by immunohistochemistry in the hiPSC GPCCi001-A cell line (C). The median, interquartile range (IQR) and mean (as diamond) are marked on the plots.

## ORCID iDs

Ewelina Stelcer  <https://orcid.org/0000-0003-0077-9539>  
 Karol Jopek  <https://orcid.org/0000-0002-7399-0303>  
 Małgorzata Blatkiewicz  <https://orcid.org/0000-0001-5506-2397>  
 Anna Olechnowicz  <https://orcid.org/0000-0001-6043-5637>  
 Kacper Kamiński  <https://orcid.org/0000-0003-0641-1444>  
 Marta Szyszka  <https://orcid.org/0000-0003-0150-3665>  
 Wiktoria Maria Suchorska  <https://orcid.org/0000-0003-4742-2465>  
 Marcin Ruciński  <https://orcid.org/0000-0002-2525-5777>

## References

- Mete O, Erickson LA, Juhlin CC, et al. Overview of the 2022 WHO Classification of Adrenal Cortical Tumors. *Endocr Pathol.* 2022;33(1):155–196. doi:10.1007/s12022-022-09710-8
- Libé R. Adrenocortical carcinoma (ACC): Diagnosis, prognosis, and treatment. *Front Cell Dev Biol.* 2015;3:45. doi:10.3389/fcell.2015.00045
- Tsai WH, Chen TC, Dai SH, Zeng YH. Case report: Ectopic adrenocortical carcinoma in the ovary. *Front Endocrinol (Lausanne).* 2021;12:662377. doi:10.3389/fendo.2021.662377
- Wang T, Rainey WE. Human adrenocortical carcinoma cell lines. *Mol Cell Endocrinol.* 2012;351(1):58–65. doi:10.1016/j.mce.2011.08.041
- Alyateem G, Nilubol N. Current status and future targeted therapy in adrenocortical cancer. *Front Endocrinol (Lausanne).* 2021;12:613248. doi:10.3389/fendo.2021.613248
- Nicolson NG, Korah R, Carling T. Adrenocortical cancer cell line mutational profile reveals aggressive genetic background. *J Mol Endocrinol.* 2019;62(4):179–186. doi:10.1530/JME-18-0262
- Cheng JY, Brown TC, Murtha TD, et al. A novel FOXO1-mediated dedifferentiation blocking role for DKK3 in adrenocortical carcinogenesis. *BMC Cancer.* 2017;17(1):164. doi:10.1186/s12885-017-3152-5
- Parmar J, Key RE, Rainey WE. Development of an adrenocorticotropin-responsive human adrenocortical carcinoma cell line. *J Clin Endocrinol Metab.* 2008;93(11):4542–4546. doi:10.1210/jc.2008-0903
- Sigala S, Rossini E, Abate A, Tamburello M, Bornstein SR, Hantel C. An update on adrenocortical cell lines of human origin. *Endocrine.* 2022;77(3):432–437. doi:10.1007/s12020-022-03112-w
- Nanba K, Blinder AR, Rainey WE. Primary cultures and cell lines for in vitro modeling of the human adrenal cortex. *Tohoku J Exp Med.* 2021;253(4):217–232. doi:10.1620/tjem.253.217
- Sigala S, Bothou C, Penton D, et al. A comprehensive investigation of steroidogenic signaling in classical and Nex experimental cell models of adrenocortical carcinoma. *Cells.* 2022;11(9):1439. doi:10.3390/cells11091439
- Sonoyama T, Sone M, Honda K, et al. Differentiation of human embryonic stem cells and human induced pluripotent stem cells into steroid-producing cells. *Endocrinology.* 2012;153(9):4336–4345. doi:10.1210/en.2012-1060
- Xing Y, Lerario AM, Rainey W, Hammer GD. Development of adrenal cortex zonation. *Endocrinol Metab Clin North Am.* 2015;44(2):243–274. doi:10.1016/j.ecl.2015.02.001
- Gordon J, Wilson VA, Blair NF, et al. Functional evidence for a single endodermal origin for the thymic epithelium. *Nat Immunol.* 2004;5(5):546–553. doi:10.1038/ni1064
- Yiangou L, Ross ADB, Goh KJ, Vallier L. Human pluripotent stem cell-derived endoderm for modeling development and clinical applications. *Cell Stem Cell.* 2018;22(4):485–499. doi:10.1016/j.stem.2018.03.016
- Manna PR, Huhtaniemi IT, Wang XJ, Eubank DW, Stocco DM. Mechanisms of epidermal growth factor signaling: Regulation of steroid biosynthesis and the steroidogenic acute regulatory protein in mouse Leydig tumor cells. *Biol Reprod.* 2002;67(5):1393–1404. doi:10.1095/biolreprod.102.007179
- Sicard F, Ehrhart-Bornstein M, Corbeil D, et al. Age-dependent regulation of chromaffin cell proliferation by growth factors, dehydroepiandrosterone (DHEA), and DHEA sulfate. *Proc Natl Acad Sci U S A.* 2007;104(6):2007–2012. doi:10.1073/pnas.0610898104
- Kinyua AW, Doan KV, Yang DJ, et al. Insulin regulates adrenal steroidogenesis by stabilizing SF-1 activity. *Sci Rep.* 2018;8(1):5025. doi:10.1038/s41598-018-23298-2
- Willenberg HS, Haase M, Papewalis C, Schott M, Scherbaum WA, Bornstein SR. Corticotropin-releasing hormone receptor expression on normal and tumorous human adrenocortical cells. *Neuroendocrinology.* 2005;82(5–6):274–281. doi:10.1159/000093126
- Zatelli MC, Rossi R, Degli Uberti EC. Androgen influences transforming growth factor-beta1 gene expression in human adrenocortical cells. *J Clin Endocrinol Metab.* 2000;85(2):847–852. doi:10.1210/jcem.85.2.6350
- Lach MS, Wroblewska JP, Augustyniak E, Kulcenty K, Suchorska WM. A feeder- and xeno-free human induced pluripotent stem cell line obtained from primary human dermal fibroblasts with epigenetic repression of reprogramming factors expression: GPCCi001-A. *Stem Cell Res.* 2017;20:34–37. doi:10.1016/j.scr.2017.02.004
- Stelcer E, Milecka P, Komarowska H, et al. Adropin stimulates proliferation and inhibits adrenocortical steroidogenesis in the human adrenal carcinoma (HAC15) cell line. *Front Endocrinol (Lausanne).* 2020;11:561370. doi:10.3389/fendo.2020.561370
- Budna J, Chachula A, Kaźmierczak D, et al. Morphogenesis-related gene-expression profile in porcine oocytes before and after in vitro maturation. *Zygote.* 2017;25(3):331–340. doi:10.1017/S096719941700020X
- Golkar-Narenji A, Antosik P, Nolin S, et al. Gene ontology groups and signaling pathways regulating the process of avian satellite cell differentiation. *Genes (Basel).* 2022;13(2):242. doi:10.3390/genes13020242
- Rucinski M, Zok A, Guidolin D, De Caro R, Malendowicz LK. Expression of precerebellins in cultured rat calvaria osteoblast-like cells. *Int J Mol Med.* 2008;22(4):553–558. PMID:18813864.
- Stelcer E, Komarowska H, Jopek K, et al. Biological response of adrenal carcinoma and melanoma cells to mitotane treatment. *Oncol Lett.* 2022;23(4):120. doi:10.3892/ol.2022.13240
- Kassambara A, Mundt F. Factoextra: Extract and visualize the results of multivariate data analyses. <https://cran.r-project.org/web/packages/factoextra/index.html>. Accessed July 27, 2023.
- Dennis G, Sherman BT, Hosack DA, et al. DAVID: Database for annotation, visualization, and integrated discovery. *Genome Biol.* 2003;4(5):P3. PMID:12734009.
- Fresno C, Fernandez EA. RDAVIDWebService: A versatile R interface to DAVID. *Bioinformatics.* 2013;29(21):2810–2811. doi:10.1093/bioinformatics/btt487
- Gu Z, Eils R, Schlesner M. Complex heatmaps reveal patterns and correlations in multidimensional genomic data. *Bioinformatics.* 2016;32(18):2847–2849. doi:10.1093/bioinformatics/btw313
- Yu G, Wang LG, Han Y, He QY. clusterProfiler: An R package for comparing biological themes among gene clusters. *OMICS.* 2012;16(5):284–287. doi:10.1089/omi.2011.0118
- Yazawa T, Imamichi Y, Miyamoto K, Umezawa A, Taniguchi T. Differentiation of mesenchymal stem cells into gonad and adrenal steroidogenic cells. *World J Stem Cells.* 2014;6(2):203–212. doi:10.4252/wjsc.v6.i2.203
- Li L, Li Y, Sottas C, et al. Directing differentiation of human induced pluripotent stem cells toward androgen-producing Leydig cells rather than adrenal cells. *Proc Natl Acad Sci U S A.* 2019;116(46):23274–23283. doi:10.1073/pnas.1908207116
- D'Amour KA, Agulnick AD, Eliazar S, Kelly OG, Kroon E, Baetge EE. Efficient differentiation of human embryonic stem cells to definitive endoderm. *Nat Biotechnol.* 2005;23(12):1534–1541. doi:10.1038/nbt1163

35. Bogacheva MS, Harjumäki R, Flander E, et al. Differentiation of human pluripotent stem cells into definitive endoderm cells in various flexible three-dimensional cell culture systems: Possibilities and limitations. *Front Cell Dev Biol.* 2021;9:726499. doi:10.3389/fcell.2021.726499
36. Kopper O, Benvenisty N. Stepwise differentiation of human embryonic stem cells into early endoderm derivatives and their molecular characterization. *Stem Cell Res.* 2012;8(3):335–345. doi:10.1016/j.scr.2011.12.006
37. Fang Y, Li X. A simple, efficient, and reliable endoderm differentiation protocol for human embryonic stem cells using crotonate. *STAR Protoc.* 2021;2(3):100659. doi:10.1016/j.xpro.2021.100659
38. Kim PTW, Hoffman BG, Plesner A, et al. Differentiation of mouse embryonic stem cells into endoderm without embryoid body formation. *PLoS One.* 2010;5(11):e14146. doi:10.1371/journal.pone.0014146
39. Tu X, Zhang Q, Zhang W, Zou X. Single-cell data-driven mathematical model reveals possible molecular mechanisms of embryonic stem-cell differentiation. *Math Biosci Eng.* 2019;16(5):5877–5896. doi:10.3934/mbe.2019294